

# Geomagnetic variations induced by the partial solar eclipse of November 25, 2011

Juan A. LAZZÚS<sup>1,2,\*</sup> , Ignacio SALFATE<sup>1</sup> 

<sup>1</sup> Departamento de Física, Universidad de La Serena, La Serena, Chile

<sup>2</sup> Instituto de Investigación Multidisciplinario en Ciencias y Tecnología,  
Universidad de La Serena, La Serena, Chile

**Abstract:** We examine the geomagnetic variations observed from the SAMBA network during the partial solar eclipse on November 25, 2011, in Antarctica. The eclipse reached nearly 90% obscuration in the western Antarctic Peninsula at the point of greatest eclipse at 06:21 UTC. Six magnetic ground stations distributed across Chile and Antarctica, around 0° longitude and at various latitudes, were used to collect geomagnetic field data in X, Y, and Z coordinates at a 1-second resolution. A baseline from the international Q-days of the month was applied to filter out isolated signals caused by the eclipse. Results indicated a systematic decrease in both the X and Y components, synchronized with the passage of the penumbra.

**Key words:** partial solar eclipse, geomagnetic field, geomagnetic fluctuations, SAMBA network, solar-terrestrial interactions, Antarctica, Chile

## 1. Introduction

When the Moon aligns between the Earth and the Sun during an eclipse, it obstructs solar radiation and can induce perturbations in the Earth's atmosphere, ionosphere, and geomagnetic field, offering a unique opportunity for scientific investigation. This transient phenomenon is classified as total (TSE), annular (ASE), or partial (PSE), depending on the extent of solar disk coverage. However, the rarity of eclipses in regions with geophysical monitoring stations limits the availability of high-resolution observational data.

The impact of solar eclipses on the Earth's environment has been extensively studied across multiple disciplines. One of the key areas of investigation is the effect on the ionosphere, particularly the decay in total electron content (TEC) due to reduced ionization caused by the temporary absence

---

\*corresponding author, e-mail: jlazzus@userena.cl

of solar ultraviolet (UV) and extreme ultraviolet (EUV) radiation (e.g. *Kumar et al., 2013; Jenan et al., 2021*). Additionally, solar eclipses have been linked to the generation of gravity waves, which propagate through the atmosphere as a response to localized cooling and subsequent pressure variations (*Jakowski et al., 2008; Chen et al., 2011*). Moreover, meteorological effects such as changes in temperature, wind patterns, and cloud formation have been reported during eclipse events (e.g. *Akimov and Chernogor, 2010; Aplin et al., 2016; Ilić et al., 2018; Lazzús et al., 2022*).

Beyond atmospheric effects, solar eclipses have been identified as external perturbations that induce variations in the Earth's geomagnetic field. These changes are attributed to modifications in ionospheric currents and alterations in the interaction between the solar wind and the Earth's magnetosphere (*Chapman, 1933; Hvoždara and Prigancová, 2002; Meza et al., 2022*). Several studies have documented significant deviations in the X and Y components of the geomagnetic field during total and partial solar eclipses. For example, *Malin et al. (2000)*, *Střeštík (1999)*, and *Özcan and Aydoğdu (2004)* reported variations of up to 10 nT in the geomagnetic field during the TSE of August 11, 1999, in Europe. *Bencze et al. (2007)* further analysed a twofold decrease in the intensity of geomagnetic pulsations during the same eclipse, both within and around the totality zone. *Momani et al. (2011)* observed a sharp decrease of  $-10$  nT in the X component with no significant changes in the Y and Z components during the TSE of November 23, 2003, in Antarctica.

Further investigations have examined geomagnetic variations across different eclipse events. *Adushkin et al. (2007)* reported fluctuations in the X component, declination, and inclination of the geomagnetic field during the TSE in Russia on March 29, 2006. Additionally, *Ateş et al. (2011)* and *Onovughe (2013)* detected an anomalous decrease in geomagnetic field intensity during the same event in Turkey. *Ladyšin et al. (2011)* found reductions of approximately  $-10$  nT in the X component and an increase in inclination during the TSE of August 1, 2008, in Russia. *Ateş et al. (2015)* reported another anomalous decrease in geomagnetic field intensity during the PSE in Turkey on January 4, 2011. Also, studies by *Ruhimat et al. (2016)* documented that the X component of geomagnetic variation decreased by up to 5 nT, while the Y component increased during the PSE in Indonesia on March 9, 2016. In contrast, *Zubaidah et al. (2016)* reported reductions

of 10 nT in the X and Y components, while the Z component increased, for the same eclipse. Additionally, *Kim and Chang (2018a, 2018b, 2018c)* demonstrated simultaneous decreases and increases in the X and Y components, respectively, using data from multiple geomagnetic observatories within the International Real-time Magnetic Observatory Network (INTERMAGNET). The most recent observations by *Vega-Jorquera et al. (2021)* in Chile reported changes of approximately 12 nT in all components of the geomagnetic field during the TSE of July 2, 2019. Also, *Lazzús (2022; 2023)*, have documented different changes in the geomagnetic field during different solar eclipses in Chile and Antarctica sector, demonstrating the diverse nature of these effects across different locations and times. Note that the discrepancies in the effects on the components of the geomagnetic field, as reported in the studies mentioned, can be attributed to several factors. Geographical differences, such as variations in the strength of the local magnetic field and latitude, affect the observations of geomagnetic changes. Furthermore, the timing and duration of the eclipse influence the magnetic field variations, as different phases of the event may produce different results. Other factors, such as local atmospheric and ionospheric conditions, can also influence these geomagnetic variations. These factors suggest that further analysis of the effects of eclipses is needed to establish a more detailed comparative analysis, considering all these methodologies and locations to fully understand these discrepancies.

On November 25, 2011, a PSE occurred over Antarctica, offering a rare chance to examine its effects on the geomagnetic field. This study utilizes data from six ground-based magnetic stations that are part of the South American Meridional B-Field Array (SAMBA), strategically positioned in Chile and Antarctica, to analyse the PSE's influence on the geomagnetic field. The positioning of these stations is crucial, as it spans different geographical locations, allowing for a comprehensive analysis of how the eclipse may have influenced the geomagnetic field across a range of latitudes. Furthermore, the local time of the eclipse event, which occurred during specific daylight hours in these regions, presents a unique opportunity to study the geomagnetic response under such conditions. Despite its significance, to the best of the authors' knowledge, no studies have been published specifically on the impact of this eclipse on the geomagnetic environment.

## 2. Partial solar eclipse of November 25, 2011

The solar eclipse of November 25, 2011, was a partial eclipse, belonging to Saros cycle 123 (53 of 70), with a magnitude of 0.905 and a maximum solar obscuration of 90.5% over Antarctica. It occurred at the descending node of the Moon's orbit, when the Moon, at a geocentric distance of approximately 365,907 km, partially covered the Sun. The eclipse began at 04:23 UTC, reached its maximum at 06:21 UTC, and ended at 08:18 UTC. It was visible in the Southern Hemisphere, with the greatest coverage in Antarctica and lesser visibility in southern Africa, Tasmania, and New Zealand. Figure 1 provides a detailed map using an orthographic projection to illustrate the path of the eclipse. This map highlights the trajectory of the eclipse, indicating the areas where the event was visible and the varying degrees of obscuration experienced at different locations.

On the other hand, it is pertinent to clarify the space weather conditions during this event. Notably, before, during, and after the eclipse, the geomagnetic conditions exhibited slight variations without indicating significant disturbances. Before the eclipse, the interplanetary magnetic field (IMF) had a magnitude of 5.7 nT, with stable components, while the solar wind had a density of  $4.7 \text{ cm}^{-3}$  and a speed of 385 km/s. The geomagnetic indices reflected low activity, with Dst at  $-9 \text{ nT}$  and Kp values of 2o, 1-, 0+, 2-, 3o, 2-, 2o, and 3-. During the eclipse, the IMF magnitude slightly decreased to 5.4 nT, with variations in  $B_y$  and  $B_z$ , while the solar wind density dropped to  $4.1 \text{ cm}^{-3}$  and its speed increased to 403 km/s. Since the Kp values were 2+, 2o, 1+, 0+, 0+, 0+, 0+, and 2-, geomagnetic activity decreased; however, Dst reaching  $-12 \text{ nT}$  indicates a subtle intensification. After the eclipse, the IMF magnitude decreased to 4.6 nT, while the solar wind density increased to  $4.8 \text{ cm}^{-3}$  and its speed decreased to 388 km/s. The geomagnetic indices recorded Dst at  $-4 \text{ nT}$ , with Kp values of 1-, 0+, 1o, 1o, 1o, 1-, 1o, and 2-. Additionally, during the same days, the daily averages of the ap and F10.7 indices showed values of 4 nT and 130, respectively. Regarding the orientation of the interplanetary magnetic field, the  $B_z$  component recorded an average negative value of  $-0.3 \text{ nT}$  (southward-oriented) on the day before the eclipse. In contrast, both the eclipse day and the following day registered an average positive value of 0.8 nT (northward-oriented), indicating a more stable behaviour in the mag-

netosphere. To clarify, the IMF and solar wind parameters were obtained from OMNIWeb (<https://omniweb.gsfc.nasa.gov/>) using measurements from the ACE and Wind satellites. The Kp index was taken from the GFZ Helmholtz Centre for Geosciences (<https://kp.gfz-potsdam.de/>), and the Dst index was obtained from Kyoto's World Data Center for Geomagnetism (<https://wdc.kugi.kyoto-u.ac.jp/>). Overall, solar activity was relatively low, a key factor in understanding the potential geomagnetic effects observed during this PSE. This low activity created optimal conditions for isolating the eclipse's effect on the geomagnetic field.

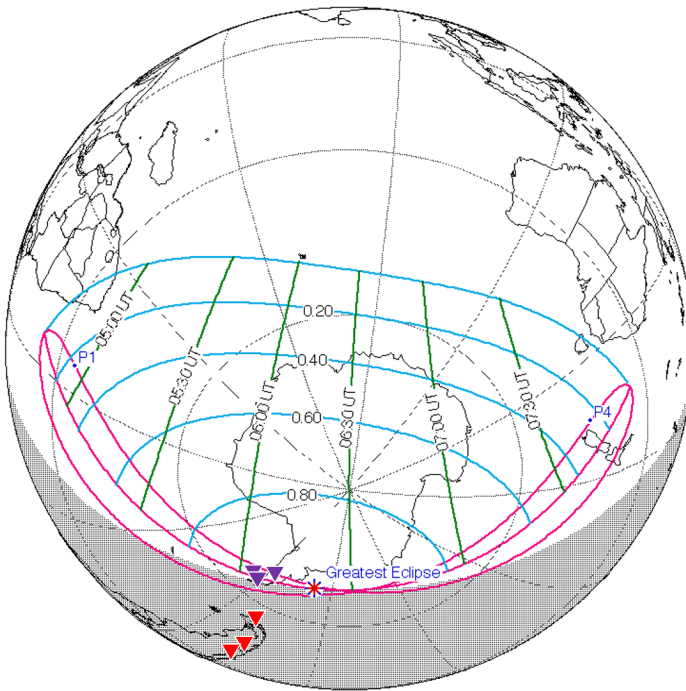


Fig. 1. Map with the orthographic projection of the PSE on November 25, 2011. The graphic shows obscuration levels and times (UTC) along the eclipse path. P1 denotes the beginning of the partial eclipse, while P4 marks its end. Additionally, the inverted triangles indicate the locations of the SAMBA stations involved in this study. From Antarctica to Chile (or from mid to low geomagnetic latitudes), the stations are: Palmer (PLMR), O'Higgins (OHI), Escudero (ESC), Punta Arenas (PAC), Osorno (OSNO), and Cerrillos (CER). Image modified from NASA's Eclipse Web Site (<https://eclipse.gsfc.nasa.gov/>).

### 3. Instruments and database

We used six stations from the South American Meridional B-Field Array (SAMBA) to investigate the geomagnetic response during the PSE. This network of magnetic stations is strategically distributed across Chile and Antarctica, covering a broad range of geomagnetic latitudes from  $-5^\circ$  to  $-50^\circ$  and around  $0^\circ$  geomagnetic longitude (*Boudouridis and Zesta, 2007*). To precisely record variations in the Earth's magnetic field, SAMBA employs three-component fluxgate magnetometers, capable of measuring the X (North), Y (East), and Z (Down) components of the geomagnetic field. These measurements are conducted at a 1-second temporal resolution, allowing for the detection of subtle fluctuations in the intensity and direction of the magnetic field during the eclipse (data is available on the SAMBA website: <http://magnetometers.bc.edu/>). Additionally, due to its geographic distribution, these stations provide essential coverage for studying these disturbances. The location of three stations on the Antarctic Peninsula coincided with the eclipse path, experiencing a magnitude greater than 0.87. Notably, during the eclipse, these stations were on the daytime side. In contrast, the remaining stations, located in Chile, were on the nighttime side during the eclipse but still within the eclipse trajectory (see Fig. 1). This variability in conditions among the selected stations is essential for identifying possible eclipse-induced disturbances and distinguishing these effects from other geomagnetic variations of external origin. Table 1 summarizes the specific eclipse conditions for the SAMBA stations used in this study.

To analyse the geomagnetic effects of the eclipse, these stations continuously recorded data before, during, and after the event. A total of 86,400 data points per day were collected to capture temporal variations of each component of the geomagnetic field. To separate eclipse induced variations from background geomagnetic activity, a baseline method was applied (e.g. *Yamazaki et al., 2011*). This approach involved selecting the 10 quietest international Q days of the same month to establish an average reference for typical geomagnetic conditions. By subtracting this baseline from the data recorded on the eclipse day, we effectively isolated the geomagnetic disturbances specifically associated with the eclipse, using a similar method to the one used in determining AE indices (*Kamei et al., 1986*).

Table 1. Details of each SAMBA station involved in this study. Columns 3 to 5 present the geographic and magnetic coordinates, while columns 6 to 9 provide the eclipse circumstances.

Station/ Country	Code	Geo. Lat./ Geo. Lon.	Mag. Lat./ Mag. Lon.	L	Partial begins UTC	Max. UTC	Partial ends UTC	Magni- tude
Cerrillos Chile	CER	−33.45 −70.60	−19.80 0.75	1.13	—	—	—	—
Osorno Chile	OSNO	−40.34 −73.09	−26.39 0.27	1.25	—	—	—	—
Pta. Arenas Chile	PAC	−53.20 −70.90	−38.27 2.87	1.63	—	—	—	—
Escudero Antarctica	ESC	−62.18 −58.92	−47.17 11.45	2.18	05:15:25	06:02:24	06:50:17	0.87541
O’Higgins Antarctica	OHI	−63.32 −57.90	−48.80 12.43	2.28	05:15:22	06:02:42	06:50:57	0.87787
Palmer Antarctica	PLMR	−64.77 −64.05	−49.74 9.2	2.39	05:19:58	06:07:27	06:55:42	0.89023

#### 4. Results and discussion

Figure 2 illustrates the variations in the X (North), Y (East), and Z (Down) components of the geomagnetic field, represented as  $\Delta X$ ,  $\Delta Y$ , and  $\Delta Z$ , during the eclipse time window. To facilitate interpretation, a vertical solid line marks the moment of the greatest eclipse, which corresponds to the maximum phase of obscuration within the region of observation. Additionally, the specific time of the maximum partial eclipse for each station is indicated by a vertical dashed line, allowing for a direct comparison of the timing of geomagnetic fluctuations with the local eclipse conditions.

Using the SAMBA stations, our results allow us to study the changes in the components of the geomagnetic field during the eclipse at different magnetic latitudes. As observed, the stations located in Chile, such as CER ( $-19.80^\circ$ ), OSNO ( $-26.39^\circ$ ), and PAC ( $-38.27^\circ$ ), show minor but still noticeable changes in the signal components that coincide with the eclipse period (see Fig. 2, panels in rows a–c). Notably, these stations exhibit progressive changes across their latitudes. In these three stations, the  $\Delta X$  and  $\Delta Y$  components show a gradual decrease from the beginning of the eclipse

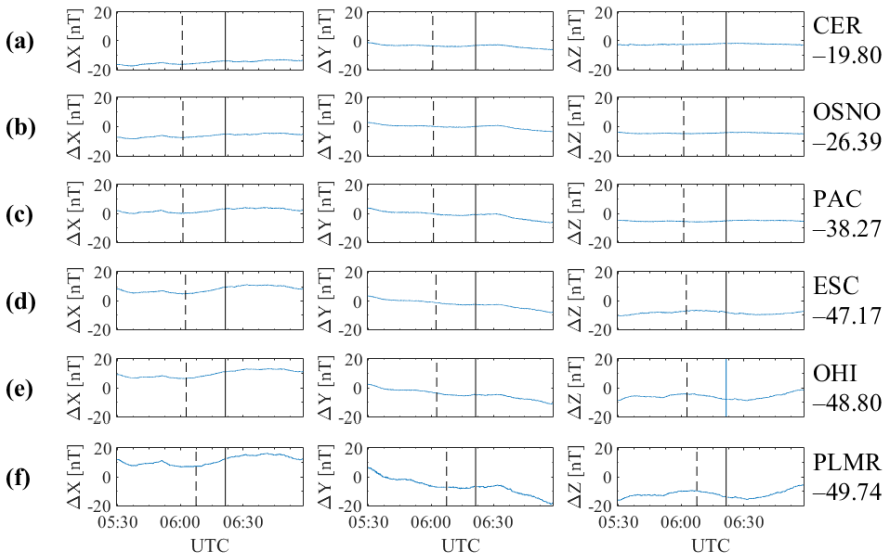


Fig. 2. Geomagnetic variations recorded during the partial solar eclipse of November 25, 2011. From left to right, the columns represent: (1st) X component, (2nd) Y component, and (3rd) Z component. From top to bottom, the rows correspond to: (a) Cerrillos (CER), (b) Osorno (OSNO), (c) Punta Arenas (PAC), (d) Escudero (ESC), (e) O’Higgins, and (f) Palmer (PLMR) stations. The vertical solid line indicates the moment of the greatest eclipse, while the vertical dashed line marks the maximum eclipse at each location. On the far right of each row, the station code and magnetic latitude for each SAMBA station are provided.

to its partial maximum, becoming more pronounced as we move from lower latitudes, such as CER ( $-19.80^\circ$ ), to mid-latitudes, such as PAC ( $-38.27^\circ$ ). In contrast, the  $\Delta Z$  component does not show any changes attributable to the eclipse at these stations.

On the other hand, the stations located in Antarctica exhibit even more significant variations in their components, which can be attributed to the eclipse. At the ESC station ( $-47.17^\circ$ ), the  $\Delta X$  and  $\Delta Y$  components also show a gradual decrease from the beginning of the eclipse to its partial maximum. During this interval, the  $\Delta X$  component decreases by approximately 6 nT, while the  $\Delta Y$  component decreases by about 4 nT, both before the moment of greatest eclipse. Additionally, the  $\Delta Z$  component shows an increase of approximately 3 nT, also coinciding with the partial maximum (see Fig. 2, panels in row d). Furthermore, the OHI ( $-48.80^\circ$ ) and PLMR

( $-49.74^\circ$ ) stations exhibit a similar but even more pronounced behaviour than that recorded at ESC within the eclipse time window. During the partial maximum, a more significant decrease is observed in both the  $\Delta X$  and  $\Delta Y$  components, with values reaching up to  $-10$  nT. At the same time, the  $\Delta Z$  component shows an increase of approximately  $5$  nT during the partial maximum at both stations (see Fig. 2, panels in rows e–f).

It should be noted that the behaviour of the three components is more complex than the dominant trends previously described. In the panels of Figure 2, there are moments that interrupt the gradual decrease or increase of the components at  $\sim 05:50$  and  $\sim 06:32$  UTC. In Figure 2, column 1, an initial decrease in  $\Delta X$  is observed, followed by a temporary increase at  $\sim 05:50$ , and then another decrease, reaching a minimum at the time of maximum eclipse at each station. Similarly,  $\Delta Y$  shows a gradual decrease, followed by a slight temporary increase at  $\sim 05:50$ , before resuming its progressive decline to a minimum at the time of maximum eclipse (see Fig. 2, column 2). In contrast,  $\Delta Z$  begins with a gradual increase, reaching a minimum at  $\sim 05:50$ , exhibiting an inverse behaviour compared to the other components (see Fig. 2, column 3). We hypothesize that this particular feature observed at  $\sim 05:50$  UTC could be a localized effect or a transient characteristic related to eclipse dynamics. Possible contributing factors include ionospheric disturbances or localized geomagnetic fluctuations that momentarily influenced the signals of the geomagnetic components (e.g., *Meza et al., 2021; Meza et al., 2022*). On the other hand, at  $\sim 06:32$  UTC, this may mark the end of the maximum eclipse for this sector. The reason why a rapid recovery to pre-eclipse conditions is not observed after this point, but rather a more pronounced evolution of the mentioned trends for each component, is that ionization levels and atmospheric dynamics require time to recover, leading to lingering effects on ionospheric currents and geomagnetic fields even after the eclipse has ended (*Chapman 1933*).

In general, our results show a contrasting behaviour between the  $\Delta X/\Delta Y$  components and the  $\Delta Z$  component at all stations, in complete synchrony with the penumbra. In addition, the path of the eclipse can be mapped across different latitudes by tracking the changes observed in the component graphs. This systematic decrease in the  $\Delta X/\Delta Y$  components suggests a direct influence of the eclipse on horizontal geomagnetic field variations, likely driven by ionospheric disturbances (see Fig. 2, panels in columns 1–2).

In contrast, the  $\Delta Z$  component exhibits a continuous increase as the eclipse progresses across the stations (see Fig. 2, panel in column 3). This trend indicates a gradual shift in geomagnetic field dynamics, potentially linked to changes in ionospheric currents or modifications in the electrodynamic coupling between different atmospheric layers due to eclipse-induced temperature variations, which influence the vertical magnetic field component (Meza *et al.*, 2021; Meza *et al.*, 2022). Furthermore, a comparative analysis of the geomagnetic field data during the days preceding and following the eclipse, within the same time window, confirms the absence of anomalies. Additionally, a careful examination of external influences during the observation period confirms that no significant solar or geomagnetic disturbances, instrumental malfunctions, or other extrinsic factors were present that could have affected the recorded geomagnetic field variations. This reinforces the conclusion that the observed variations in the  $\Delta X$ ,  $\Delta Y$ , and  $\Delta Z$  components are directly related to the eclipse and not to other transient geomagnetic phenomena.

When comparing our results with similar analyses of other solar eclipses over the Chile and Antarctica sector, we observe both consistencies and notable differences. Lazzús (2022) reported a pattern similar to the one observed in this study during the total solar eclipse of July 11, 2010, where both the X and Y components decreased, while the Z component increased. In contrast, Lazzús (2023) observed a different response during the partial solar eclipse of September 11, 2007, with a decrease in the X component, an increase in the Y component, and a flattening of the Z component signal. Notably, the differences in the behaviour of certain components, particularly the Y and Z components, suggest that distinct observational conditions played a key role in shaping geomagnetic responses. For instance, the 2010 eclipse ended at dusk, with the Sun at an altitude of approximately  $1^\circ$  above the horizon. This low solar elevation likely influenced ionospheric conductivity and geomagnetic variations. Conversely, the 2007 eclipse occurred around noon, when the Sun was at its maximum altitude, leading to a different ionospheric response. For the eclipse analysed in this study, it took place at dawn with an altitude of  $\sim 1^\circ$ , where this condition likely produced a response similar to that of the 2010 eclipse.

Accordingly, Stankov *et al.* (2017) emphasize that geomagnetic variations during a solar eclipse are influenced by multiple interrelated factors. These

include the geographic location of the observation site, seasonal effects, and the extent of solar radiation reduction. The interplay of these factors affects the dynamics of ionospheric currents, leading to variations in the geomagnetic field that differ across eclipse events. One of the most critical factors is the geographic location of the stations, as the stations at different latitudes may experience distinct responses depending on their position relative to the path of the umbra and penumbra (*Lazzús, 2023*). Seasonal effects also play a crucial role in shaping the geomagnetic response. The ionospheric conductivity varies throughout the year due to changes in solar zenith angle and atmospheric composition, particularly in the distribution of ionized particles. Furthermore, the degree of solar radiation reduction during an eclipse directly impacts ionospheric electrodynamics (*Jenan et al., 2021*). A total eclipse results in a more significant drop in ionospheric electron density compared to a partial eclipse, leading to more pronounced disruptions in geomagnetic field components. This distinction may explain why past eclipse studies report differences in geomagnetic signals.

On the other hand, the results obtained for this eclipse (see Fig. 2) align well with the theoretical predictions proposed by *Chapman (1933)*, which describe how the temporary reduction in solar radiation during an eclipse alters ionospheric conductivity. Specifically, our results agree with the prediction that the sudden loss of solar radiation during an eclipse causes localized cooling in the ionosphere, as ion production depends on solar UV radiation. This decrease in ionization leads to changes in conductivity, which in turn modify the ionospheric dynamo, resulting in temporary perturbations in the geomagnetic field consistent with the eclipse event. Additionally, several researchers have documented similar effects, further validating the results of this study (some examples can be found in Section 1). These reports confirm that geomagnetic field variations during solar eclipses follow a predictable pattern, with fluctuations in the horizontal ( $\Delta X$  and  $\Delta Y$ ) and vertical ( $\Delta Z$ ) components linked to ionospheric disturbances. More recent research, including works by *Momani et al. (2011)*, *Ateş et al. (2011)*, *Ladynin et al. (2011)*, and *Babakhanov et al. (2013)*, have demonstrated that the magnitude and duration of geomagnetic perturbations depend on factors such as eclipse geometry and ionospheric conditions.

Given this, it is reasonable to attribute the detected variations to the so-called “*lunar shield*” effect. This phenomenon describes the temporary

obstruction of solar radiation by the Moon, which disrupts the normal ionospheric balance. As solar radiation is momentarily blocked, the ionization levels in the ionosphere decrease, leading to reduced conductivity. This, in turn, alters the prevailing ionospheric currents, which play a crucial role in generating geomagnetic field variations. As the eclipse progresses and solar radiation returns to normal levels, the ionosphere gradually recovers, restoring the typical geomagnetic field configuration (see Fig. 2).

## 5. Conclusions

The study of the November 25, 2011, partial solar eclipse provides further evidence of the direct influence of solar eclipses on geomagnetic field variations, reinforcing the link between solar radiation, ionospheric currents, and geomagnetic fluctuations. To analyse these effects, data were collected from six SAMBA network magnetic stations strategically positioned at different magnetic latitudes around the  $0^\circ$  geomagnetic longitude and within the eclipse's penumbra. These stations enabled a comparative analysis of geomagnetic responses at different latitudes during the eclipse. The X, Y, and Z components of the geomagnetic field were examined relative to a baseline and analysed during the eclipse's time window.

This analysis led to several important conclusions regarding the influence of the eclipse on the geomagnetic field:

- 1) A systematic decrease in both the X and Y components was observed during the eclipse, reaching a minimum near the partial maximum. The Z component exhibited an increase, contrasting with the behaviour of the other components.
- 2) No significant solar or geomagnetic disturbances were detected during the observation period, ruling out external sources as potential contributors to the observed variations. Additionally, a careful verification of instrumental performance confirmed that no malfunctions affected the recorded data.
- 3) All detected changes in the geomagnetic field components can be directly attributed to the lunar shield effect, where the Moon's temporary obstruction of solar radiation modifies ionospheric conductivity and influences geomagnetic field dynamics.

- 4) The results presented here are consistent with both theoretical predictions and prior observational studies, further supporting the established understanding of solar eclipses' impact on geomagnetic variations.

**Acknowledgements.** The authors thank the Direction of Research and Development of the University of La Serena (DIDULS) and the Department of Physics of the University of La Serena (DFULS) for their support in the preparation of this paper. Special thanks go to E. Yizengaw, E. Zesta, M. B. Moldwin, and the rest of the SAMBA team for providing the data, as well as NASA's Eclipse Web Site for Fig. 1.

## References

- Adushkin V. V., Gavrilov B. G., Gorelyi K. I., Rybnov Y. S., Kharlamov V. A., 2007: Geophysical effects of the March 29, 2006, solar eclipse. *Dokl. Earth Sci.*, **417**, 2, 1393–1397, doi: 10.1134/S1028334X07090218.
- Akimov A. L., Chernogor L. F., 2010: Effects of the solar eclipse of August 1, 2008, on the Earth's lower atmosphere. *Kinemat. Phys. Celest. Bodies*, **26**, 3, 135–145, doi: 10.3103/S0884591310030050.
- Aplin K. L., Scott C. J., Gray S. L., 2016: Atmospheric changes from solar eclipses. *Philos. Trans. R. Soc. A*, **374**, 2077, 20150217, doi: 10.1098/rsta.2015.0217.
- Ateş A., Büyüksaraç A., Bektaş Ö., 2011: Geophysical variations during the total solar eclipse in 2006 in Turkey. *Turk. J. Earth Sci.*, **20**, 3, 337–342, doi: 10.3906/yer-0906-14.
- Ateş A., Ekinci Y. L., Buyuksarac A., Aydemir A., Demirci A., 2015: Statistical analysis of geomagnetic field variations during the partial solar eclipse on 2011 January 4 in Turkey. *Res. Astron. Astrophys.*, **15**, 5, 742–752, doi: 10.1088/1674-4527/15/5/011.
- Babakhanov I. Y., Belinskaya A. Y., Bizin M. A., Grekhov O. M., Khomutov S. Y., Kuznetsov V. V., Pavlov A. F., 2013: The geophysical disturbances during the total solar eclipse of 1 August 2008 in Novosibirsk, Russia. *J. Atmos. Sol.-Terr. Phys.*, **92**, 1–6, doi: 10.1016/j.jastp.2012.09.016.
- Bencze P., Heilig B., Zieger B., Szendroi J., Verő J., Lühr H., Yumoto K., Tanaka Y., Stréšník J., 2007: Effect of the August 11, 1999 total solar eclipse on geomagnetic pulsations. *Acta Geod. Geophys. Hung.*, **42**, 1, 23–58, doi: 10.1556/ageod.42.2007.1.2.
- Boudouridis A., Zesta E., 2007: Comparison of Fourier and wavelet techniques in the determination of geomagnetic field line resonances. *J. Geophys. Res. Space Phys.*, **112**, A8, A08205, doi: 10.1029/2006JA011922.
- Chapman S., 1933: The effect of a solar eclipse on the Earth's magnetic field. *Terr. Magn. Atmos. Electr.*, **38**, 3, 175–183, doi: 10.1029/TE038i003p00175.
- Chen G., Zhao Z., Zhang Y., Yang G., Zhou C., Huang S., Li T., Li N., Sun H., 2011: Gravity waves and spread *Es* observed during the solar eclipse of 22 July 2009. *J. Geophys. Res. Space Phys.*, **116**, A9, A09314, doi: 10.1029/2011JA016720.

- Hvoždara M., Prigancová A., 2002: Geomagnetic effects due to an eclipse-induced low-conductivity ionospheric spot. *J. Geophys. Res. Space Phys.*, **107**, A12, 1467, doi: 10.1029/2002JA009260.
- Ilić L., Kuzmanoski M., Kolarž P., Nina A., Srećković V., Mijić Z., Bajčetić J., Andrić M., 2018: Changes of atmospheric properties over Belgrade, observed using remote sensing and in situ methods during the partial solar eclipse of 20 March 2015. *J. Atmos. Sol.-Terr. Phys.*, **171**, 250–259, doi: 10.1016/j.jastp.2017.10.001.
- Jakowski N., Stankov S. M., Wilken V., Borries C., Altadill D., Chum J., Buresova D., Boska J., Sauli P., Hruska F., Cander Lj. R., 2008: Ionospheric behavior over Europe during the solar eclipse of 3 October 2005. *J. Atmos. Sol.-Terr. Phys.*, **70**, 6, 836–853, doi: 10.1016/j.jastp.2007.02.016.
- Jenan R., Dammalage T. L., Panda S. K., 2021: Ionospheric total electron content response to September-2017 geomagnetic storm and December-2019 annular solar eclipse over Sri Lankan region. *Acta Astronaut.*, **180**, 575–587, doi: 10.1016/j.actaastro.2021.01.006.
- Kamei T., Araki T., Sugiura M., 1986: Auroral Electrojet Indices (AE) for July-December 1983, Data Book No. 13, World Data Center C2 for Geomagnetism, Kyoto, Japan, available at [https://wdc.kugi.kyoto-u.ac.jp/wdc/pdf/indexplot/13%20Aurora1%20electrojet%20indices%20\(AE\)%20for%20July-December%201983.pdf](https://wdc.kugi.kyoto-u.ac.jp/wdc/pdf/indexplot/13%20Aurora1%20electrojet%20indices%20(AE)%20for%20July-December%201983.pdf).
- Kim J.-H., Chang H.-Y., 2018a: Statistical analysis of geomagnetic field variations during solar eclipses. *Adv. Space Res.*, **61**, 8, 2040–2049, doi: 10.1016/j.asr.2018.01.022.
- Kim J.-H., Chang H.-Y., 2018b: Geomagnetic field variations observed by INTERMAGNET during 4 total solar eclipses. *J. Atmos. Sol.-Terr. Phys.*, **172**, 107–116, doi: 10.1016/j.jastp.2018.03.023.
- Kim J.-H., Chang H.-Y., 2018c: Geomagnetic field variations during solar eclipses and the geographic location of observing sites. *J. Korean Astron. Soc.*, **51**, 4, 119–127, doi: 10.5303/jkas.2018.51.4.119.
- Kumar S., Singh A. K., Singh R. P., 2013: Ionospheric response to total solar eclipse of 22 July 2019 in different Indian regions. *Ann. Geophys.*, **31**, 9, 1549–1558, doi: 10.5194/angeo-31-1549-2013.
- Ladynin A. V., Semakov N. N., Khomutov S. Y., 2011: Changes in the daily geomagnetic variation during the total solar eclipse of 1 August 2008. *Russ. Geol. Geophys.*, **52**, 3, 343–352, doi: 10.1016/j.rgg.2011.02.007.
- Lazzús J. A., 2022: Geomagnetic response to the total solar eclipse on 11 July 2010 in Chile. *Geomagn. Aeron. (Engl. Transl.)*, **62**, 5, 652–656, doi: 10.1134/S0016793222050085.
- Lazzús J. A., 2023: Geomagnetic effects of the partial solar eclipse of 11 September 2007 in Chile and Antarctica. *Geomagn. Aeron. (Engl. Transl.)*, **63**, 4, 497–502, doi: 10.1134/S0016793223600029.
- Lazzús J. A., Vega-Jorquera P., Pacheco R., Tamblay L., Martínez-Ledesma M., Ovalle E. M., Carrasco E., Bravo M., Villalobos C. U., Salfate I., Palma-Chilla L., Foppiano A. J., 2022: Changes in meteorological parameters during the total solar eclipse of 2 July 2019 in La Serena, Chile. *Ann. Geophys.*, **65**, 5, PA531, doi: 10.4401/ag-8623.

- Malin S. R. C., Özcan O., Tank S. B., Tunçer M. K., Yazıcı-Çakın O., 2000: Geomagnetic signature of the 1999 August 11 total eclipse. *Geophys. J. Int.*, **140**, 3, F13–F16, doi: 10.1046/j.1365-246X.2000.00061.x.
- Meza A., Eylonstein B., Natali M. P., Bosch G., Moirano J., Chalar E., 2021: Analysis of ionospheric and geomagnetic response to the 2020 Patagonian solar eclipse. *Front. Astron. Space Sci.*, **8**, 766327, doi: 10.3389/fspas.2021.766327.
- Meza A., Bosch G., Natali M. P., Eylonstein B., 2022: Ionospheric and geomagnetic response to the total solar eclipse on 21 August 2017. *Adv. Space Res.*, **69**, 1, 16–25, doi: 10.1016/j.asr.2021.07.029.
- Momani M. A., Al Smadi T. A., Al Taweel F. M., Ghaidan K. A., 2011: Magnetic field disturbances during the 2003 total solar eclipse over Antarctica as observed by magnetometers. *Eur. J. Technol. Adv. Eng. Res.*, **2**, 2, 69–75.
- Onovughe E. V., 2013: Geomagnetic diurnal variation during the total solar eclipse of 29 March 2006. *Int. J. Astron.*, **2**, 4, 51–55, doi: 10.5923/j.astronomy.20130204.01.
- Özcan O., Aydoğdu M., 2004: Possible effects of the total solar eclipse of August 11, 1999 on the geomagnetic field variations over Elazığ-Turkey. *J. Atmos. Sol.-Terr. Phys.*, **66**, 11, 997–1000, doi: 10.1016/j.jastp.2004.03.009.
- Ruhimat M., Winarko A., Nuraeni F., Bangkit H., Aris M. A., Suwardi, Sulimin, 2016: Effect of March 9, 2016 total solar eclipse on geomagnetic field variation. *J. Phys. Conf. Ser.*, **771**, 012036, doi: 10.1088/1742-6596/771/1/012036.
- Stankov S. M., Bergeot N., Berghmans D., Bolsée D., Bruyninx C., Chevalier J.-M., Clette F., De Backer H., De Keyser J., D’Huys E., Dominique M., Lemaire J. F., Magdalenic J., Marqué C., Pereira N., Pierrard V., Sapundjiev D., Seaton D. B., Stegen K., Van der Linden R., Verhulst T. G. W., West M. J., 2017: Multi-instrument observations of the solar eclipse on 20 March 2015 and its effects on the ionosphere over Belgium and Europe. *J. Space Weather Space Clim.*, **7**, A19, doi: 10.1051/swsc/2017017.
- Střeštík J., 1999: The response of the 11 August 1999 total solar eclipse in the geomagnetic field. *Earth Moon Planets*, **85–86**, 561–566, doi: 10.1023/A:1017047627850.
- Vega-Jorquera P., Lazzús J. A. Tamblay L., Palma-Chilla L., Salfate I., Pacheco R., 2021: Geomagnetic field variations during the total solar eclipse of July 2019 in La Serena, Chile. *Geomagn. Aeron. (Engl. Transl.)*, **61**, 2, 287–292, doi: 10.1134/S0016793221020171.
- Yamazaki Y., Yumoto K., Cardinal M. G., Fraser B. J., Hattori P., Kakinami Y., Liu J. Y., Lynn K. J. W., Marshall R., McNamara D., Nagatsuma T., Nikiforov V. M., Otadoy R. E., Ruhimat M., Shevtsov B. M., Shiokawa K., Abe S., Uozumi T., Yoshikawa A., 2011: An empirical model of the quiet daily geomagnetic field variation. *J. Geophys. Res. Space Phys.*, **116**, A10, A10312, doi: 10.1029/2011JA016487.
- Zubaidah T., Kanata B., Paniran P., Wiriasto G. W., 2016: Observation of geomagnetic fields changes related to 9th March 2016 solar eclipse on Lombok Island-Indonesia. In: *Proc. 7th Indonesia Japan Joint Scientific Symposium*, 20–24 November, Chiba, Kanto, Japan, available at <https://opac.ll.chiba-u.jp/da/curator/107920/ceresIntlSympo-24-P875.pdf>.